Low-Cost Implementation of PV-STATCOM for Non-Linear Load Using STM32F407VG Controller

Nimita Gajjar[1], Tejas Zaveri[2], Naimish Zaveri[3]

[1]*Associate Professor, Dept. of Electrical Engineering, GEC Surat, India, GTU research scholar*
[2]*GTU research supervisor, India*
[3]*Professor, Department of Electrical Engineering, CKPCET Surat, India*

[1]nimita_gajjar@hotmail.com, [2] tejas1009@gmail.com, [3] naimish.zaveri@ckpcet.ac.in

Abstract — *This paper presents the low-cost hardware implementation of solar inverter-based STATCOM for correction of power factor in case of non-linear industrial load. It explores the multifunctionality of PV inverters to not only deliver real power but to deal with other power quality issues like poor power factor due to non-linear load. This multifunctionality is achieved in the daytime with the capacity of the inverter remaining after supplying PV power to the load/grid. At night time, the full capacity of the inverter is available for grid support functionalities. In the developed prototype, the decoupled control techniques were implemented using the STM32 microcontroller. A modified SOGI based estimator is used to find grid voltage angle as well as the reactive component of the load current. Experiments are done for various conditions of load and variable solar insolation, and results are discussed to validate the proposed system.*

Keywords — *DSTATCOM, decoupled control, Distributed Generation, Photovoltaic system, Smart Inverter, Unity Power Factor operation, Voltage Control.*

I. INTRODUCTION

Solar power in India, as well as the world, is fast emerging in the renewable energy sector in the past few years as it supports sustainable growth while fulfilling the needs of the nation's energy sector and assurance for energy security. According to the ministry of new & renewable energy, a total of 40 GW installed capacity of solar plants is available across India as of 31-03-2021. The Mission targets to install grid-connected solar power plants with a capacity of up to 100 GW by the year 2022. To achieve the above target, various schemes have been launched by the Government of India. Canal bank & Canal top Scheme, CPSU Scheme, Solar Park Scheme, Defence Scheme, VGF Schemes, and Grid Connected Solar Rooftop Scheme, etc., are launched to encourage the generation of solar power in the country which receives solar energy for the most part of the year [1]. Millions of people in India and across the globe have benefited from solar energy-based decentralized and distributed applications. Their energy needs such as lighting, agriculture, commercial, and others are met in a sustainable and environmentally friendly manner. There is a very vast market for solar in India, and due to various schemes & subsidies, it is already gearing up.

Presently with a grid-connected solar plant or roof-top system, it focuses only on injecting active power into the grid& there is no consideration of reactive power requirement and issues like poor power factor & steady-state voltage variation. With challenges in the integration of solar PV with grid, like temporary/steady-state over-voltages and harmonics, etc. Also, varying environmental conditions worsen these problems as it injects variable solar power into the system. For maintaining the required power quality level, there are standards and codes like IEEE-519 and IEEE-1547. So there is a need to maintain the power quality within limits as per the standards. In literature, we may find many devices and methods for improving power quality. The idea of utilizing the PV-inverter as STATCOM in the nighttime was proposed back in 2009 [2], which can be used to improve power quality with little or no additional cost. Many control techniques and configurations were proposed in the literature for the STATCOM [3]-[7]. Verma et al. have demonstrated LVRT (low-voltage ride through) capacity of PV-STATCOM in which PV inverter reduces active power injection into the grid for a short period of time during disturbance and renders all of its energy available for reactive power support [8], [9]. Singh et al. have implemented various control techniques based on LMS (least means square) algorithm [10]-[12]. Various MPPT techniques are also reported in literature like P & O, InC, fuzzy logic, variable step size incremental, etc.[13]-[15], which enables the user to choose according to the application. Power quality improvement for different load conditions using PV-DSTATCOM or wind STATCOM was presented in [16]-[17]. Based on the above literature review, this paper contributes to the development of PV-STATCOM for mitigation of harmonics and maintaining unity power factor for industrial loads employing non-linear rectifier loads without much cost. The LT industries having critical non-linear rectifier loads are mainly focused on maintaining UPF at their end, and also, a reduction in harmonics is desirable. The proposed system proposes a low-cost and effective solution for achieving UPF as well as harmonic reduction.

The main objective of this paper is to supply active power to the connected load at the PCC as well as into the grid while deriving maximum power from PV module using P & O MPPT technique, to develop PV-STATCOM for the solution of power quality issues like poor power factor & harmonics caused by non-linear loads and to develop second-order generalized (SOGI) based estimators for the reduced need of voltage sensors and to employ DC blocker along with SOGI estimators and thereby increases the stability of grid angle estimation.

In this paper, the system configuration and different modes of operation are described in section II. The control scheme description and design are covered in section III. In section IVsexperimental results are discussed, and lastly, the conclusion is discussed in Section V.

II. SYSTEM DESCRIPTION AND DESIGN

The schematic configuration of the proposed system is as depicted in fig 1. Grid-connected PV system (single-stage) is considered with non-linear load is connected at PCC. The PV-inverter is acting as STATCOM to supply

When PV generation is low $P_{pv} < P_L$, the load is then supplied with active power from both the grid and the PV inverter.

In addition to active power, the load's reactive power needs can be fulfilled by the PV inverter while keeping the unity power factor. When PV power is available, the inverter can fulfill both active & reactive power requirements of load; however, when PV power is unavailable at night, only reactive power can be provided.

A. Control scheme

The control scheme is as depicted in fig. 2. P & O MPPT algorithm is implemented to get maximum power. A modified SOGI (second-order generalized integrator) estimator is used for grid angle estimation with reduced voltage sensors. Only one voltage sensor is used for estimating grid angle by using SOGI-frequency locked loop (SOGI-FLL). A detailed explanation of the control scheme is as below.

reactive power needed by non-linear load and improve power quality. For practical laboratory setup & operation of the grid-connected system, fig. 1 also illustrates the number of sensors needed for sensing various parameters. Four AC sensors are used for sensing grid voltage & currents. Three sensors for load current and two DC sensors for sensing DC link voltage V_{dc} & PV current I_{pv}. The sensed signals (voltage and current)are passed through the control block to generate reference signals for switching of inverter depending on required functionalities. Under variable solar insolation, the power output of the SPV array is also variable, and therefore for maximum power extraction from the SPV module, the perturb and observe algorithm is implemented.

The active power needed by the non-linear load connected at PCC is met by the grid as well as PV-inverter depending on the output from the SPV array throughout the day. When the extracted PV power (P_{pv}) is greater than the active power required by load (P_L), then surplus power is supplied to the grid.

a) P & O MPPT algorithm: Perturb & Observe MPPT algorithm is used owing to its simplicity & less computational complexity. In this algorithm for tracking of maximum PV power, DC bus voltage is controlled. As depicted in fig. 3 the voltage perturbation of the PV module should be increased toward the MPP if the PV module's operating point is on the LHS of the P-V curve ($\Delta P_{pv}/\Delta V_{dc}$ is +ve), indicating that the PV module power is rising. If the module's operating point is on the RHS of the curve ($\Delta P_{pv}/\Delta V_{dc}$ is -ve), the voltage perturbation should be reduced toward the MPP. The DC link voltage is either decreased or increased depending on the sign of slope $\Delta P_{pv}/\Delta V_{dc}$. If this slope is positive, then V_{dc} is increased by δV_{dc} and vice versa.
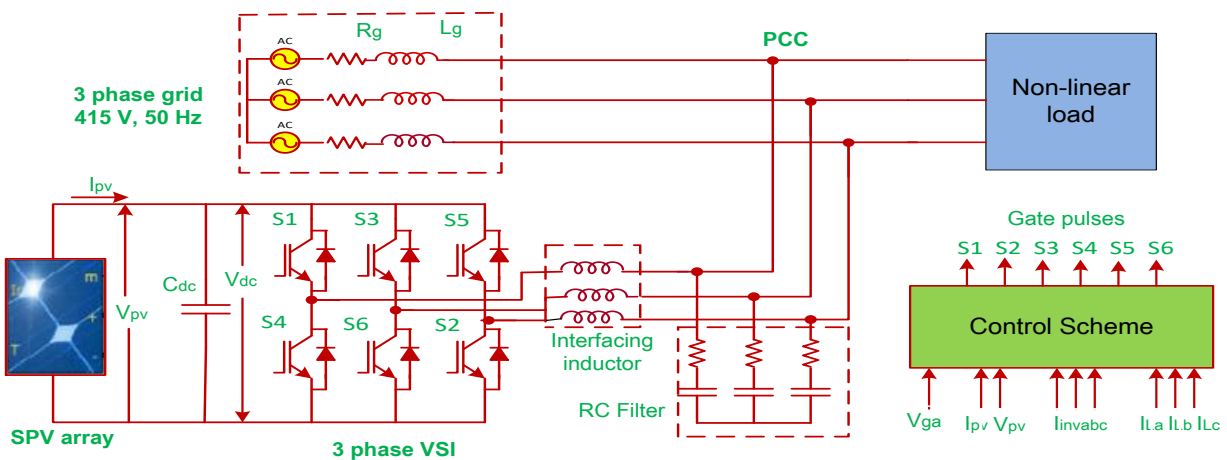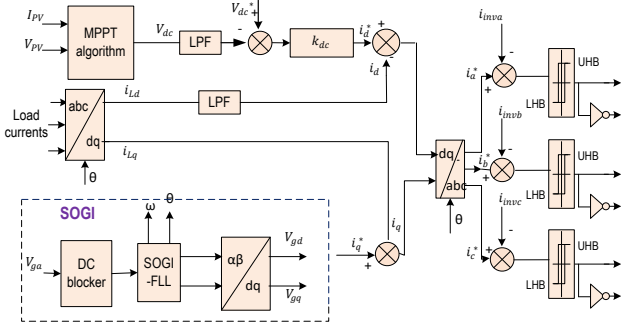

Fig. 1 Schematic configuration of the proposed system

Fig. 2 Decoupled control of the system

Fig 3. PV curve of solar panel

b) SOGI-FLL estimator: Nowadays, digital controllers come with a single-ended ADC (analog to digital converter) on the chip. The on-chip single-ended ADC generates an output that corresponds to the signal's positive value. Before any further processing on this output, a DC offset should be added to it. When this DC-biased output signal is processed using the traditional SOGI approach, it then becomes unstable [18-19]. A modified SOGI method is used here, which is realized by using conventional SOGI with DC blocker, as shown in fig. 4. The cascading digital differentiator and integrator are used to implement the DC blocker. The DC blocker transfer function is governed by the following equation.

$$H(s) = \frac{-s+1}{p_{dc} \; s+1} \qquad (1)$$

A zero is added to nullify the effect of DC offset, and a pole is added to eliminate the pole's differentiation effect on the input signal. The pole's location is a tradeoff between bandwidth and transient response. For optimum performance, the value of P_{dc} should be selected between 0.95 to 0.998 [19]. To ensure good filtering and minimum attenuation, in the presented work, P_{dc} is selected as 0.998. The filtered output in discrete time is given as

$$v_{gaf}[m] = v_{gaf}[m-1]p_{dc} + v_{ga}[m] - v_{ga}[m-1] \quad (2)$$

where v_{ga} represents grid voltage and v_{gaf} is filtered voltage. The grid voltage angle is estimated using orthogonal components of grid voltage.
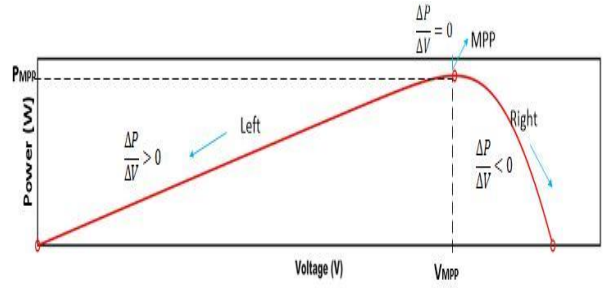
$$\theta_v[m] = tan^{-1}\left(\frac{v_{\beta g}[m]}{v_{\alpha g}[m]}\right) \qquad (3)$$

$$v_{g\alpha}[m] = v_{g\alpha}[m-1] + \left[e_v[m] \cdot k_v - v_{g\beta}[m]\right] \cdot \left[\omega[m-1] \cdot T_s\right] \qquad (4)$$

$$v_{g\beta}[m] = v_{g\beta}[m-1] + v_{g\alpha}[m] \cdot \omega[m-1] \cdot T_s \quad (5)$$

$$\omega_m = \omega_{m-1} - \lambda_\omega \cdot v_{g\beta}[m] \cdot e_v[m] \cdot T_s \qquad (6)$$

Where $v_{g\alpha}$, $v_{g\beta}$ are orthogonal components of voltage, θ_v is the estimated grid angle, ω is the frequency of the grid, T_s is sampling time, and $k_v \& \lambda_\omega$ represents SOGI-FLL gain.

The s domain representation of transfer function for direct and quadrature output of SOGI is given by

$$\frac{Y(s)}{U(s)} = \frac{k \cdot \omega_0 \cdot s}{s^2 + k \cdot \omega_0 \cdot s + \omega_0^2} \qquad (7)$$

$$\frac{Y\prime(s)}{U(s)} = \frac{k \cdot \omega_0^2}{s^2 + k \cdot \omega_0 \cdot s + \omega_0^2} \qquad (8)$$

here k is the constant of proportionality (k_{is} or k_{vs}). As shown in fig. 5 (bode plot diagram), a higher value of k response is faster, but bandwidth is smaller and vice-versa. Hence k is selected such that optimum speed and filtering is achieved. For the practical purpose, it is selected between 1 to 1.4.
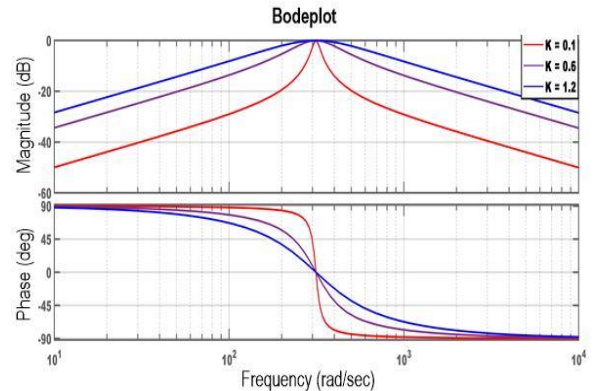
Fig 4 Bodeplot for different values of k

c) VSI control

Decoupled DQ control: At any given PCC voltage, the inverter's active & reactive power can be governed by d & q components respectively of inverter current [9]. The direct and quadrature axis components of VSI current can be found by eq. 9.

As shown in fig. 4, by controlling the direct (d) axis current loop, active power can be regulated. Where the reference current of the d axis (i^*_{ddc})is obtained by the DC bus voltage regulator, the P & O algorithm is implemented to obtain the dc-link reference voltage (v^*_{dc}), which is then compared to the actual dc link voltage (v_{dc}). The error signal (v_{der}) is then passed through PI regulator. Its digital implementation is as per eq. 10.

$$\begin{bmatrix} f_d(m) \\ f_q(m) \end{bmatrix} = \frac{2}{3} \begin{bmatrix} cos\,\emptyset[m] & cos\left[\emptyset[m] - \frac{2\pi}{3}\right] & cos\left[\emptyset[m] + \frac{2\pi}{3}\right] \\ sin\,\emptyset[m] & sin\left[\emptyset[m] - \frac{2\pi}{3}\right] & sin\left[\emptyset[m] + \frac{2\pi}{3}\right] \end{bmatrix} \begin{bmatrix} f_a[m] \\ f_b[m] \\ f_c[m] \end{bmatrix} \tag{9}$$

$$i^*_{ddc}[m] = i^*_{ddc}[m-1] + k_p \cdot (v_{der}[m] - v_{der}[m-1]) \cdot (k_i \cdot T_c \cdot v_{der}[m]) \tag{10}$$

The PV inverter can also supply reactive power with the remaining capacity after converting active power. The reference PV inverter current is selected for unity power factor operation.

$$i^*_q[m] = -i_{qL}[m] \tag{11}$$

The reactive component of the inverter current should be equal to the reactive component of load such that no reactive power is drawn from the grid.
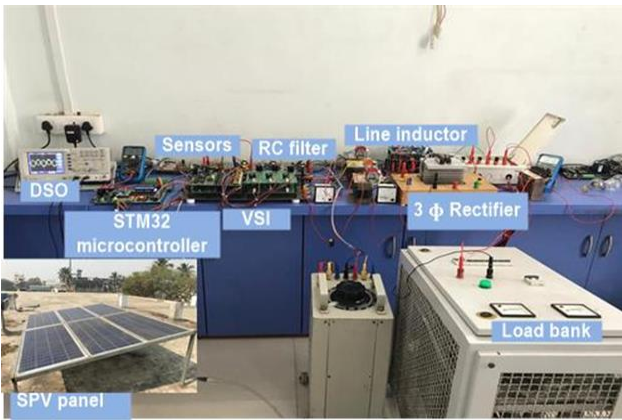
III. EXPERIMENT SETUP

Fig. 5 Laboratory setup of the system

The laboratory setup of the presented system is as depicted in fig. 5. The 3 Φ grid of 400V, 50Hz is stepped down to 110V by an autotransformer. A line inductance of 5 mH is connected to a 110V supply to realize the transmission line, which is then supplying power to the non-linear load at PCC. The PV module consists of six 150 Wp PV arrays (Waree make) connected in series (total of 900 Wp). PV array is connected to a three-phase two-level VSI (voltage source inverter). An RC filter is connected after VSI for the reduction of switching frequency ripples. To sense various parameters like grid voltage, DC bus voltage, load current, and PV current, a Hall Effect sensor card (NiTech made) is used. ARM-CORTEX M4 microcontroller(STM32F407VG) is used to process the sensed signals with the proposed control scheme. Hysteresis control (a variable frequency control approach) is dependent on characteristics such as hysteresis bandwidth, load, and input voltage, but it has better dynamics when implemented in a digital system [20]. The variable-frequency disadvantage is avoided by altering the sampling period of the ADC. Constant frequency in hysteresis control can be performed by adjusting the sampling period of the ARM cortex microcontroller's analog to digital converter to a fixed value. Under various system operating modes, the proposed system is tested in both conditions, i.e., steady-state and dynamic conditions.

IV. RESULTS & DISCUSSION

The presented test system is tested under different operating modes under conditions of steady-state and dynamic. Results are shown to validate the effectiveness of the SOGI-FLL system for estimation of grid voltage angle and extraction of decoupled components V_d & V_q (at different values of PV power) for PV to grid interface. The exchange of reactive power for unity power factor operation while supplying active power is also demonstrated. In all the modes, the grid voltage (line to line) is set to a value of 110 V rms, and reference DC link voltage is varied from 235 V to 270 V depending on the PV power. The experimental outcome for different modes is discussed in the following subsections. Rating of various components used in the laboratory setup of the system is as outlined in *Appendix A*.

A. Mode I (PV to grid mode)

Only active power is transmitted from PV to grid/loading this mode. The SOGI-FLL is utilized to calculate grid voltage angle and produce stationary reference frame (SRF) voltages. The estimated parameters are studied for dynamic and steady-state conditions. For a steady-state change in PV power, the predicted angle using SOGI-FLL is illustrated in fig.7. Figure 8 shows the dynamic performance of SOGI-FLL estimators in PV to grid mode as solar irradiance changes dynamically. Fast estimation of SOGI parameters is desirable to attain stable grid-connected operation under transient conditions. As PV power increases (due to an increase in irradiance) from 660W to 1150W, which is clear from fig.7, grid current is increasing as the PV source is feeding more power to the grid. The system operates like a traditional PV system injecting generated PV power (active power) into the grid; therefore, power flows reverses in the grid. The d axis component of VSI current follows the reference to transfer PV power to the grid and maintain the voltage of the DC link. The VSI reactive power is zero; therefore, the reactive current is maintained at zero value.

As is evident from fig.7, when PV power is 660W, grid current is less, and as it changes to 1150W, more power is pumped into the grid, and it results in an increase in grid current while dc bus voltage varies from 235V to 270V. The variation in PV power was achieved by using semi-transparent material to shade the PV array.
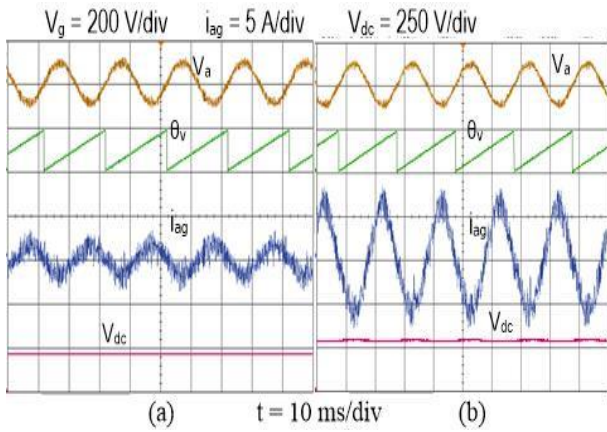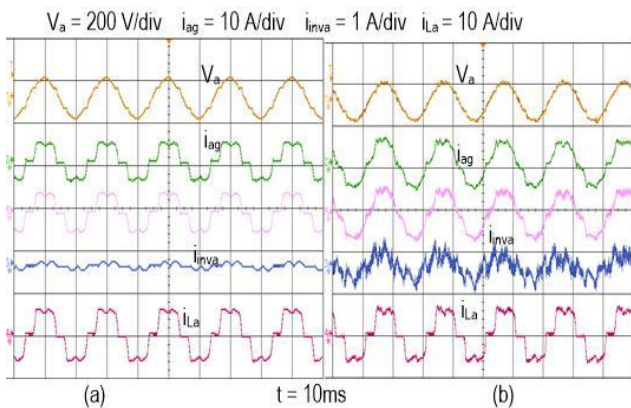
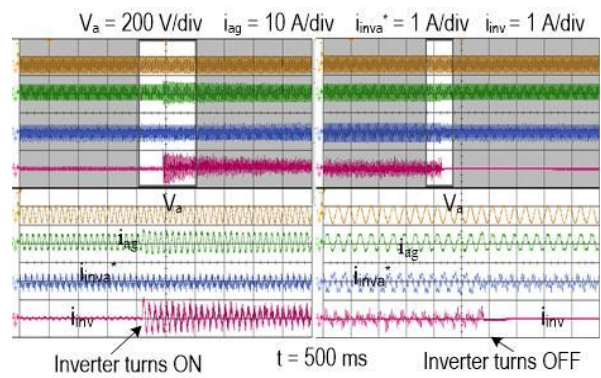**Fig. 6 Performance of SOGI estimator under different PV power**
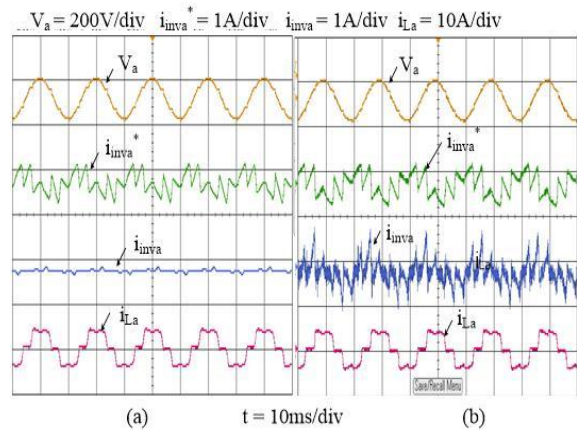
Fig 8 System performance in mode II
(a) before compensation   (b) after compensation
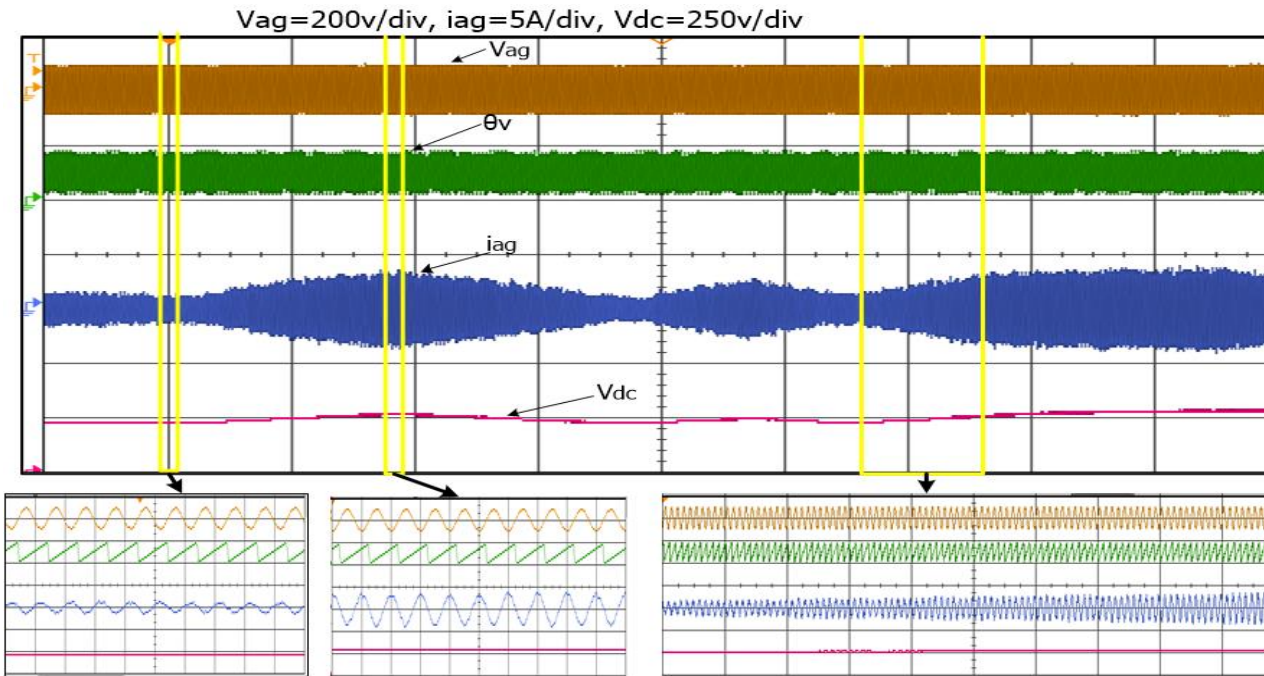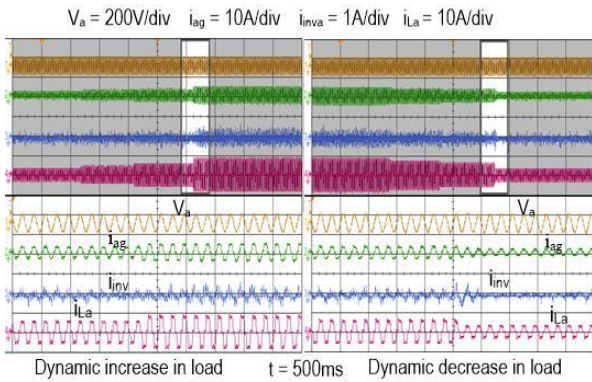

Fig. 7 Dynamic performance under variable PV power

Fig 9 Effect on grid current in mode II (a) before compensation   (b) after compensation

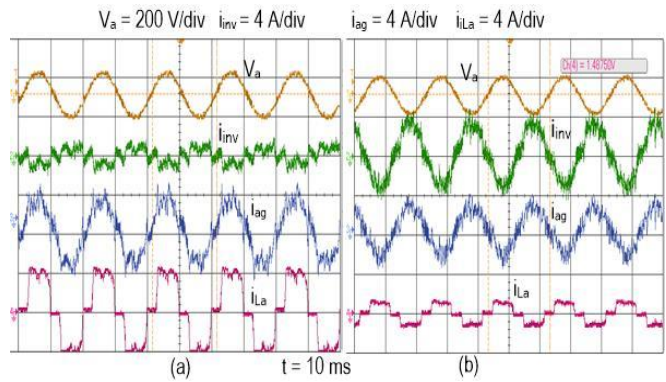**Fig 10 Dynamic performance in mode II**

Fig 11. System performance under dynamic load change condition (mode II).

Fig 12 System performance in mode III (a)for high load requirement and low PV power (b) for low load requirement and high PV power

B. Mode II (Nighttime mode):

When PV power either is not available in nighttime or in the daytime when weather is cloudy and not enough PV power is generated. The PV inverter is still used as an active filter to mitigate harmonics by exchanging required reactive power. The inverter uses all of its capacity to supply reactive power as active power is zero. The active power requirement of the load is managed by the grid. Figure 9 shows the change in current of the inverter as observed before as well as after the compensation. Inverter current closely follows the reference current, which shows the effectiveness of the control system. Figure 10 shows grid current before and after compensation. Before compensation, the reactive power is supplied by the grid. Therefore the grid current is non-linear& distorted, but after compensation, it becomes nearly sinusoidal, as the reactive power requirement of the load is taken care of by the PV inverter. Figure 11 shows the dynamic condition of suddenly starting and stopping compensation. It is shown that the inverter current follows the reference smoothly. Figure 12 shows the dynamic change in load current. Grid current changes as it is supplying active power, but it is maintained sinusoidal as PV inverter manages reactive power.

C. Mode III (Combined mode):

In this mode, the VSIfed the active power generated by PV array to grid/load and also supplies reactive power demand of the connected load. It thus acts as STATCOM, also compensating load reactive power requirement and maintaining UPF at point of common coupling. Fig. 13(a) shows the condition for high PV generation and low load requirement. As load power requirement is less than available PV power, the surplus power is injected into the grid, and thus the power flow is reversed in the grid. Fig. 13(b) shows a condition of low PV generation and high load requirement. Active power of the load is now supplied from PV as well as grid. Figure 14 depicts the dynamic load variation from 5A to 0A, and the PV inverter is supplying both active.
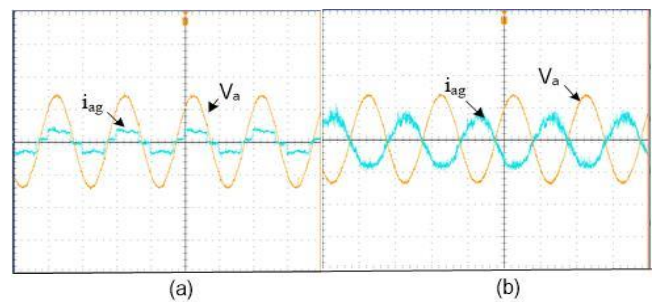
Fig 13 UPF operation of STATCOM (a) before compensation (b) after compensation

Reactive power as required by the load. Fig. 15 shows power factor correction mode as the system is supplying not only active power to the load but also taking care of its reactive power demand. The grid absorbs the surplus power, as shown in fig 15 by the shift in grid current direction (the grid current is now in 180^0 phase opposition to grid voltage as well as its sinusoidal). Also the unity power factor operation does not affect the active power transfer by VSI. It demonstrates the effective decoupled operation of active and reactive power.

V. CONCLUSION

The proposed scheme has been used for a multifunctional PV module connected with the three-phase grid. The system is quite suitable for LT industrial applications, especially where the nonlinear load of the rectifier is used as these loads are critical loads, the reliability of power can be maintained to the grid and the load. The presented system is developed using an STM32 microcontroller, and no DSPACE or any other expensive controller is used. The use of a SOGI estimator and a low-cost STM32 microcontroller proposes a cost-effective system with more reliability. The utilization of the PV inverter system is greatly improved. The proposed PV system can solve power quality issues in distributed generation caused due to non-linear loads. The presented test results have authenticated the robustness and feasibility of the proposed PV system under various modes and make it a suitable choice for LT industrial applications.

REFERENCES

[1]   Ministry of New and Renewable Energy-India website), Available from https://mnre.gov.in/solar , (2021).

[2]   R. K. Varma, V. Khadkikar, and R. Seethapathy, Nighttime application of pv solar farm as statcom to regulate grid voltage, IEEE transactions on energy conversion, 24(4) (2009) 983–985.

[3]   B. Singh, P. Jayaprakash, D. P. Kothari, A. Chandra, and K. Al Haddad, "Comprehensive study of dstatcom configurations, IEEE Transactions on Industrial Informatics,10(2) (2014) 854–870.

[4]   Q.-N. Trinh and H.-H. Lee, An enhanced grid current compensator for a grid-connected distributed generation under nonlinear loads and grid voltage distortions, IEEE Transactions on Industrial Electronics, 61(12) (2014) 6528–6537.

[5]   S. Mishra and P. K. Ray, Power quality improvement using photovoltaic fed dstatcom based on Jaya optimization, IEEE Transactions on Sustainable Energy, 7(4) (2016) 1672–1680.

[6]   C. Kumar and M. K. Mishra, A multifunctional dstatcom is operating under stiff source, IEEE Transactions on Industrial Electronics, 61(7) (2013) 3131–3136.

[7]   C. Kumar and M. K. Mishra, Operation and control of an improved performance interactive dstatcom, IEEE transactions on industrial electronics, 62(10) (2015) 6024–6034.

[8]   R. K. Varma and E. M. Siavashi, Enhancement of solar farm connectivity with smart pv inverter pv-statcom, IEEE Transactions on Sustainable Energy, 10(3) (2018) 1161–1171.

[9]   R. K. Varma and E. M. Siavashi, Pv-statcom: A new smart inverter for voltage control in distribution systems, IEEE Transactions on Sustainable Energy, 9(4) (2018) 1681–1691.

[10]   R. K. Agarwal, I. Hussain, and B. Singh, Implementation of llmf control algorithm for a three-phase grid-tied spv-dstatcom system, IEEE Transactions on Industrial Electronics, 64(9) (2016) 7414–7424.

[11]   B. Singh, C. Jain, and S. Goel, Ilst control algorithm of single-stage dual purpose grid connected solar pv system, IEEE Transactions on Power Electronics, 29(10) (2013) 5347–5357.

[12]   S. K. Sahoo, S. Kumar, and B. Singh, Vssmlms-based control of multifunctional pv-dstatcom system in the distribution network, IET Generation, Transmission & Distribution, 14(11) (2020) 2100– 2110.

[13]   N. Femia, G. Petrone, G. Spagnuolo, and M. Vitelli, A technique for improving p&o mppt performances of double-stage grid-connected photovoltaic systems, IEEE transactions on industrial electronics, 56(11) (2009) 4473–4482.

[14]   M. A. G. De Brito, L. Galotto, L. P. Sampaio, G. d. A. e Melo, and C. A. Canesin, Evaluation of the main mppt techniques for photovoltaic applications, IEEE transactions on industrial electronics, 60(3) (2012) 1156–1167.

[15]   Q. Mei, M. Shan, L. Liu, and J. M. Guerrero, A novel improved variable step-size incremental-resistance mppt method for pv systems, IEEE transactions on industrial electronics, 58(6) (2010) 2427–2434.

[16]   Sindhuja, P., and B. Lalitha., Reactive Power Compensation for Grid Connected Distribution System using DSTATCOM for Different Loads, International Journal of Engineering Trends and Technology (IJETT), 40(5) (2016) 257-264.

[17]   Rakhi Deshmukh, Rahul Rahangdale, M.K. Pradhan., A Power Quality Improvement By using STATCOM and Wind Turbine, International Journal of Engineering Trends and Technology, 32(6) (2016) 260-265.

[18]   K. Mozdzynski, K. Rafał, and M. Bobrowska-Rafał., Application of the second order generalized integrator in digital control systems, Archives of Electrical Engineering, 63(3) (2014).

[19]   R. Yates and R. Lyons, Dc blocker algorithms [dsp tips & tricks], IEEE Signal Processing Magazine, 25(2) (2008) 132–134.

[20]   D. Kalyanraj and S. L. Prakash, Design and digital implementation of constant frequency hysteresis current controller for three-phase voltage source inverter using tms320f2812, International Journal of Emerging Electric Power Systems, 15(1) (2014) 13–23.

Appendix A

A. SPV Parameters

Power P_{MPP} = 150W,
Voltage at MPP V_{MPP} = 36.10V ,
Current at MPP I_{MPP} = 4.16A,
Six modules connected in series for a total power output of 900W, Manufacture: Waaree,
DC bus voltage = 230V -290V,
DC bus capacitor = 2330μF

B. Grid and load paameters

Grid voltage= 415V, 50Hz,

RC Filter at PCC: R= 10ohm/10 W,
C = 2.5μF/440V
Non-Linear Load - Rectifier – IRI MDS100/16 3-Φ Full bridge Rectifier,
Line inductor= 5mH,

C. SOGI-FLL Parameters

$\lambda\omega$ = 0.1,
DC blocker = 0.998

D. Cost of components used in developing hardware

ARM Cortex controller: Rs.19900,
3 phase bridge rectifier: Rs.2200,
Sensors: Rs. 10000,
Infineon card: Rs. 26600,
DC link capacitor: Rs.1500,
inductors: Rs. 1950,
RC filter: Rs.200

Nomenclatures

e_v	Error signal
i^*_d i^*_q	Direct and quadrature axis reference current
k_p k_i	Filter constant
K_{vg}	SOGI-FLL gains
p_{dc}	Filter constant
$V_{g\alpha}$ $V_{g\beta}$	Grid voltage's orthogonal components
V_{ga}	Grid voltege
V_{gaf}	Filtered voltage
T_c	Sampling time

Greek Symbols

θ_v	Angle of grid voltage
Ω	Grid frequency (estimated)
λ_ω	SOGI-FLL gains

Abbreviations

DSTATCOM	Distribution static synchronous compensator
FLL	Frequency locked loop
LHS	Left hand side
LT	Low tension
MPPT	Maximum power point tracking
PCC	Point of common coupling
P & O	Perturb and observe
SOGI	Second order generalised integrator
RHS	Right hand side
SPV	Solar photo voltaic
UPF	Unity power factor
VSI	Voltage source inverter